

SUPPLEMENTARY INFORMATION of

**N<sub>2</sub> fixation in the Mediterranean Sea related to the composition of the diazotrophic community, and impact of dust under present and future environmental conditions**

Céline Ridame<sup>1</sup>, Julie Dinasquet<sup>2,3</sup>, Søren Hallstrøm<sup>4</sup>, Estelle Bigeard<sup>5</sup>, Lasse Riemann<sup>4</sup>, France Van Wambeke<sup>6</sup>, Matthieu Bressac<sup>7</sup>, Elvira Pulido-Villena<sup>6</sup>, Vincent Taillandier<sup>7</sup>, Fred Gazeau<sup>7</sup>, Antonio Tovar-Sanchez<sup>8</sup>, Anne-Claire Baudoux<sup>5</sup>, Cécile Guieu<sup>7</sup>

<sup>1</sup> Sorbonne University, CNRS, IRD, LOCEAN: Laboratoire d'Océanographie et du Climat: Expérimentation et Approches Numériques, UMR 7159, 75252 Paris Cedex 05, France

<sup>2</sup> Scripps Institution of Oceanography, University of California San Diego, USA

<sup>3</sup> Sorbonne University, CNRS, Laboratoire d'Océanographie Microbienne, LOMIC, 66650 Banyuls-sur-Mer, France

<sup>4</sup> Marine Biology Section, Department of Biology, University of Copenhagen, 3000 Helsingør, Denmark

<sup>5</sup> Sorbonne University, CNRS, Station Biologique de Roscoff, UMR 7144 Adaptation et Diversité en Milieu Marin, France

<sup>6</sup> Aix-Marseille Université, Université de Toulon, CNRS/INSU, IRD, Mediterranean Institute of Oceanography (MIO), UM 110, 13288, Marseille, France

<sup>7</sup> Sorbonne Université, CNRS, Laboratoire d'Océanographie de Villefranche, LOV, 06230 Villefranche-sur-Mer, France

<sup>8</sup> Department of Ecology and Coastal Management, Institute of Marine Sciences of Andalusia (CSIC), 11510 Puerto Real, Cádiz, Spain

Correspondence to: Céline Ridame (celine.ridame@locean.ipsl.fr)

Table S1: Nutrients stocks (DIP, DFe, NO<sub>3</sub><sup>-</sup>) in the surface mixed layer (SML) and in the euphotic layer (surface to the 1%PAR depth).

\* at stations 1 to 4, micromolar NO<sub>3</sub><sup>-</sup> concentrations were under detection limit (0.05 μM) in the upper 50 m and samples for the nanomolar level determination (LWCC) were lost. For these stations, maximum NO<sub>3</sub><sup>-</sup> stocks were calculated considering a concentration of 0.05 μM when NO<sub>3</sub><sup>-</sup> concentrations were under this detection limit.

	Lat.	Long.	MLD	1% PAR depth	DIP Stock SML	DFe Stock SML	NO <sub>3</sub> <sup>-</sup> Stock SML	DIP Stock euphotic	DFe Stock euphotic	NO <sub>3</sub> <sup>-</sup> Stock euphotic
	°N	°E	m	m	μmol.m <sup>-2</sup>	μmol.m <sup>-2</sup>	μmol.m <sup>-2</sup>	μmol.m <sup>-2</sup>	μmol.m <sup>-2</sup>	mmol.m <sup>-2</sup>
ST01	41.89	6.33	21	58	160	18.2	<1050*	525	45	<16.4*
ST02	40.51	6.73	21	72	227	24.0	<1050*	1277	63	<27.7*
ST03	39.13	7.68	11	85	53	24.7	<550*	1080	142	<10.3*
ST04	37.98	7.98	15	66	106	30.1	<750*	1284	113	<13.0*
ST05	38.95	11.02	9	78	112	10.9	258	1306	80	16.6
TYR	39.34	12.59	9	68	64	11.7	137	693	71	1.5
ST06	38.81	14.50	18	67	198	35.1	162	708	97	5.0
ST07	36.66	18.15	18	75	104	24.7	162	458	83	2.2
ION	35.49	19.78	14	87	142	23.4	195	982	126	1.6
ST08	36.21	16.63	14	75	169	22.2	911	950	87	5.5
ST09	38.13	5.84	7	87	77	10.0	819	1183	80	15.7
FAST	37.95	2.90	9	83	99	13.8	716	2775	94	13.1
ST10	37.45	1.57	19	87	308	22.3	2016	3187	84	28.3

Table S2: FrameBot annotations of the nearest known references of the 20 most abundant ASVs across all samples.

Feature ID	Reads	% of all reads	FrameBot annotation	% Identity
4f130f7262e949bc20ae5dcd3eee35db	247955	28,12	145569915 1G B 1 1432264_1433145_CP000304 Pseudomonas_stutzeri_A1501	98,925
00c85e66b298fa566b5587b50e7f3f7f	114420	12,97	213578830 1B B 1 FJ170277_complement_13629_14492 Uncultured_cyanobacterium_group_A_nif_cluster	100
74fc02da755a36c195bbece4dcfb6c3e	69304	7,86	213578830 1B B 1 FJ170277_complement_13629_14492 Uncultured_cyanobacterium_group_A_nif_cluster	100
3aa5d34aa2ac8a8f7506577551a510a0	65812	7,46	145569915 1G B 1 1432264_1433145_CP000304 Pseudomonas_stutzeri_A1501	98,925
9d2f4ec132745ac31c2340a031d726ee	63165	7,16	145569915 1G B 1 1432264_1433145_CP000304 Pseudomonas_stutzeri_A1501	98,925
ab0ecbee56ec313cda72e61ffdcfb494	56134	6,37	145569915 1G B 1 1432264_1433145_CP000304 Pseudomonas_stutzeri_A1501	98,925
3474fb451f8b288dcb190ddd9933884	38007	4,31	145569915 1G B 1 1432264_1433145_CP000304 Pseudomonas_stutzeri_A1501	98,925
e067e3ba7a65706248056188777e1763	27641	3,13	213578830 1B B 1 FJ170277_complement_13629_14492 Uncultured_cyanobacterium_group_A_nif_cluster	100
66b09bb28a2d6b2c8a074c7ef455abcf	25793	2,92	213578830 1B B 1 FJ170277_complement_13629_14492 Uncultured_cyanobacterium_group_A_nif_cluster	100
f60991866f34f6a2e51e132307e5bad4	19615	2,22	142330 1G B 1 525_1397_M11579 Azotobacter_vinelandii_DK_cluster_	96,774
106b2b300923c99f0a32e68826fb05c3	18111	2,05	213578830 1B B 1 FJ170277_complement_13629_14492 Uncultured_cyanobacterium_group_A_nif_cluster	100
769ab520efbbb7280f93376b03c1c171	18051	2,05	110168604 1B B 1 6380808_6381698_CP000393 Trichodesmium_erythraeum_IMS101	98,925
e48ca7a05e71d1f402f7f36cc81cb450	8525	0,97	145569915 1G B 1 1432264_1433145_CP000304 Pseudomonas_stutzeri_A1501	98,925
717a2d9ae33622985dde7cb936331c18	8214	0,93	145569915 1G B 1 1432264_1433145_CP000304 Pseudomonas_stutzeri_A1501	98,925
b5e593c3cbea96f53a5e597bd502715d	8117	0,92	145569915 1G B 1 1432264_1433145_CP000304 Pseudomonas_stutzeri_A1501	98,925
12fa8a7272c36cef116e673efd697ce5	5548	0,63	145569915 1G B 1 1432264_1433145_CP000304 Pseudomonas_stutzeri_A1501	98,925
90c741ef17c027078254972c547eaaaa	4206	0,48	142330 1G B 1 525_1397_M11579 Azotobacter_vinelandii_DK_cluster_	96,774
226e7bd030e1242d67bffeacc3dfb50a	3984	0,45	242120818 3E C 2 CP001649_complement_488297_489124 Desulfovibrio_salexigens_DSM_2638	98,925
5cd4866faf5030e82d079b211a72997b	3410	0,39	145569915 1G B 1 1432264_1433145_CP000304 Pseudomonas_stutzeri_A1501	98,925
0eabd0c5b6d4ada9c3ed3b7458a4d431	3135	0,36	145569915 1G B 1 1432264_1433145_CP000304 Pseudomonas_stutzeri_A1501	98,925

Table S3: FrameBot annotations of the nearest known references of the 20 most abundant ASVs at station 10

Feature ID	Reads	% of all	FrameBot annotation	%Identity	Taxonomic group
bbc2563311419e73e0612506d8153935	58485	39,55	213578830 1B B 1 FJ170277_complement_13629_14492 Uncultured_cyanobacterium_group_A_nif_cluster	100	UCYN-A4
74fc02da755a36c195bbece4dcfb6c3e	38889	26,30	213578830 1B B 1 FJ170277_complement_13629_14492 Uncultured_cyanobacterium_group_A_nif_cluster	100	UCYN-A1
a5ee5acfb641bc085da0aa23b0637b4e4	13007	8,80	213578830 1B B 1 FJ170277_complement_13629_14492 Uncultured_cyanobacterium_group_A_nif_cluster	100	UCYN-A4
66b09bb28a2d6b2c8a074c7ef455abc	10132	6,85	213578830 1B B 1 FJ170277_complement_13629_14492 Uncultured_cyanobacterium_group_A_nif_cluster	100	UCYN-A2
106b2b300923c99f0a32e68826fb05c3	9164	6,20	213578830 1B B 1 FJ170277_complement_13629_14492 Uncultured_cyanobacterium_group_A_nif_cluster	100	UCYN-A1
00c85e66b298fa566b5587b50e7f3f7f	5970	4,04	213578830 1B B 1 FJ170277_complement_13629_14492 Uncultured_cyanobacterium_group_A_nif_cluster	100	UCYN-A3
e067e3ba7a65706248056188777e1763	1347	0,91	213578830 1B B 1 FJ170277_complement_13629_14492 Uncultured_cyanobacterium_group_A_nif_cluster	100	UCYN-A3
0d074fa0254f3044df289a87f37c42e6	1106	0,75	213578830 1B B 1 FJ170277_complement_13629_14492 Uncultured_cyanobacterium_group_A_nif_cluster	100	UCYN-A4
f4a69bcdæa044367c837f016e3ffaec	1095	0,74	213578830 1B B 1 FJ170277_complement_13629_14492 Uncultured_cyanobacterium_group_A_nif_cluster	100	UCYN-A1
ab0ecbee56ec313cda72e61ffdcb494	1064	0,72	145569915 1G B 1 1432264_1433145_CP000304 Pseudomonas_stutzeri_A1501	98,925	Gamma proteobacteria
d2675af859c82c0d4bb46f8c3d91311d	1024	0,69	213578830 1B B 1 FJ170277_complement_13629_14492 Uncultured_cyanobacterium_group_A_nif_cluster	100	UCYN-A1
4f130f7262e949bc20ae5dcd3ee35db	948	0,64	145569915 1G B 1 1432264_1433145_CP000304 Pseudomonas_stutzeri_A1501	98,925	Gamma proteobacteria
17d5b4757a75ad4a6a6a8714e6724aeb	727	0,49	213578830 1B B 1 FJ170277_complement_13629_14492 Uncultured_cyanobacterium_group_A_nif_cluster	100	UCYN-A1
e8681f8ab1563b2921531f4d68020eb0	581	0,39	213578830 1B B 1 FJ170277_complement_13629_14492 Uncultured_cyanobacterium_group_A_nif_cluster	98,925	UCYN-A4
5cb4ec245b40a8d3760ca91743295b55	411	0,28	213578830 1B B 1 FJ170277_complement_13629_14492 Uncultured_cyanobacterium_group_A_nif_cluster	100	UCYN-A4
806cee9c1b2488bacb2a595080138b42	409	0,28	213578830 1B B 1 FJ170277_complement_13629_14492 Uncultured_cyanobacterium_group_A_nif_cluster	100	UCYN-A1
f66f288c4a3ce20feb425c205abff587	311	0,21	213578830 1B B 1 FJ170277_complement_13629_14492 Uncultured_cyanobacterium_group_A_nif_cluster	100	UCYN-A4
3aa5d34aa2ac8a8f7506577551a510a0	293	0,20	145569915 1G B 1 1432264_1433145_CP000304 Pseudomonas_stutzeri_A1501	98,925	Gamma proteobacteria
792d37be15059dfb929140300a7f7a4a	234	0,16	213578830 1B B 1 FJ170277_complement_13629_14492 Uncultured_cyanobacterium_group_A_nif_cluster	100	UCYN-A2
15464fc769f26e7ea2e0d3ee53e52a57	225	0,15	237685316 1G B 1 1597309_1598187_CP001614 Teredinibacter_turnerae_T7901	94,624	Gamma proteobacteria

Figure S1 Integrated primary production (PP) (a) and heterotrophic bacterial production (BP) (b) from surface to euphotic layer depth along the longitudinal PEACETIME transect

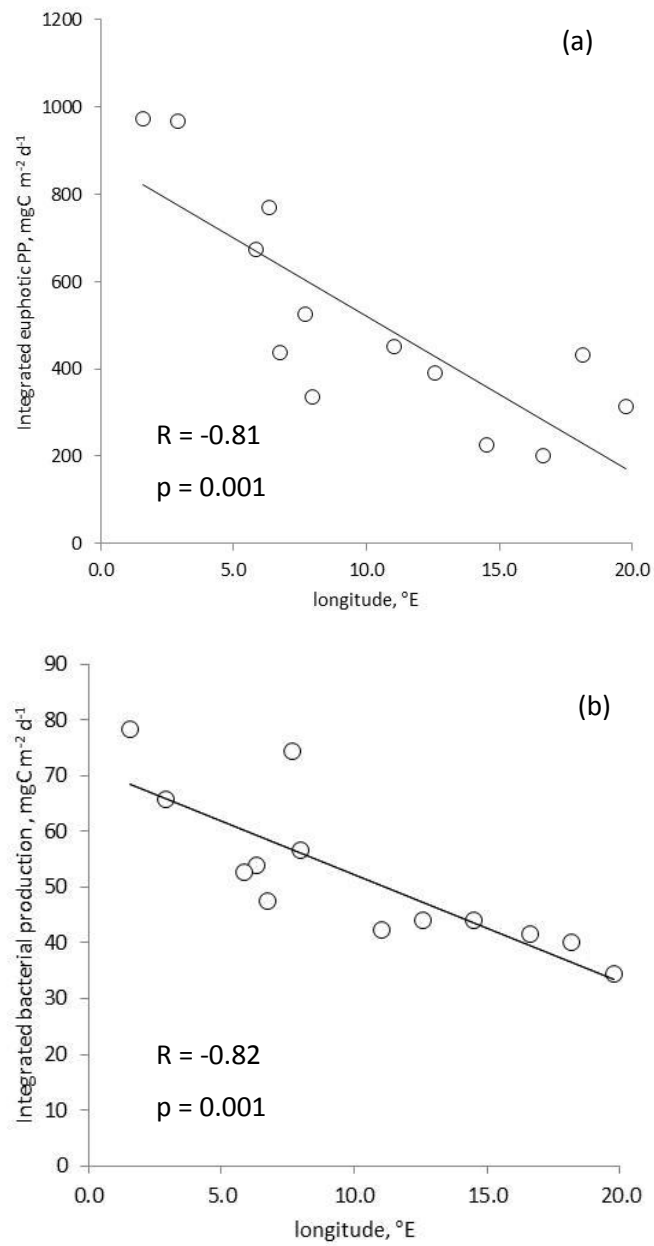


Figure S2 : Slope (and standard deviation) of N<sub>2</sub> fixation (a-c) versus time in the controls (C, black), dust treatments under present climate conditions (D, red) and dust treatments under future climate conditions (G, green) during the dust seeding experiments at TYR, ION and FAST. Only data presenting a significant linear relationship with time (Pearson's correlation coefficient,  $p < 0.05$ ) were included. Slopes that were significantly different within one experiment are labelled with different letters (A, B, C).

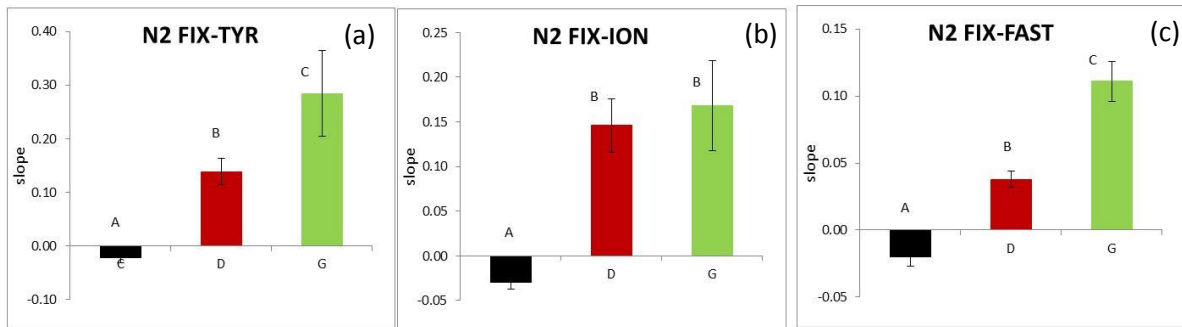


Figure S3: Box plots of the relative changes (in %) in  $^{13}\text{C}$ -primary production (PP) over the duration of the dust seeding experiments at TYR, ION, and FAST stations. D means dust treatments under present climate conditions and G dust treatments under future climate conditions.

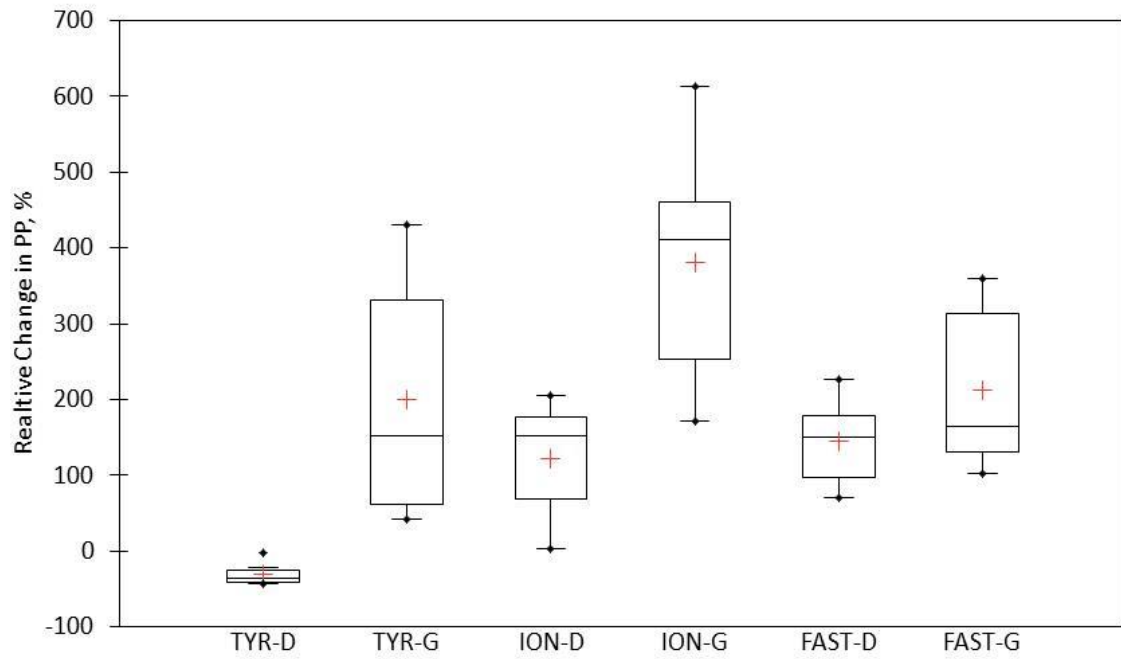


Figure S4: Principal coordinate analysis of diazotroph communities. Distances between samples were calculated as Bray-Curtis dissimilarity. Only ASVs above 1% relative abundance were included in this analysis

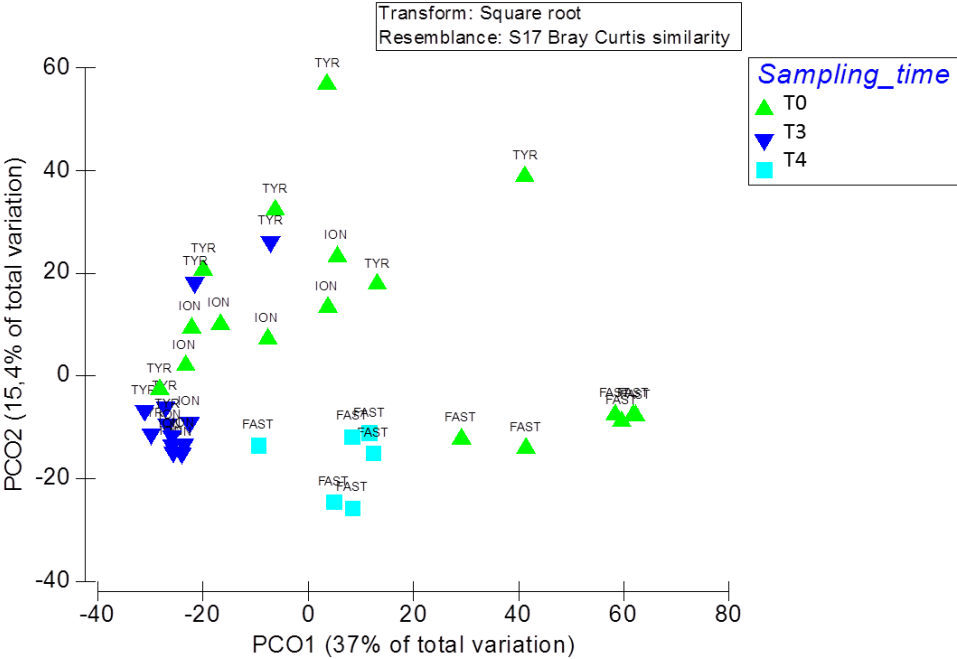




Figure S5: General diversity trends visualized by Shannon H index, at TYR, ION and FAST. Shows that for TYR and ION the diversity decrease from T0 to Tend whereas the opposite is true for FAST.

